

1 Shutting down dust emission during the middle Holocene
2 drought in central Arizona

3 **Guy Tau^{1,2*}, Onn Crouvi², Yehouda Enzel¹, Nadya Teutsch², Paul Ginoux³, and Craig**
4 **Rasmussen⁴**

5 ¹ *The Fredy & Nadine Herrmann Institute of Earth Sciences, The Hebrew University of*
6 *Jerusalem, The Edmond J. Safra Campus, Givat Ram, Jerusalem 9190401, Israel*

7 ² *Geological Survey of Israel, 32 Yeshayahu Leibowitz, Jerusalem 9692100, Israel*

8 ³ *National Ocean and Atmospheric Administration, Geophysical Fluid Dynamics Laboratory,*
9 *Princeton, NJ 08540, USA*

10 ⁴ *Department of Environmental Science, University of Arizona, Tucson, AZ 85721, USA*

11
12 **ABSTRACT**

13 Long-term relationships between climate and dust emission remain unclear, with two prevailing,
14 but opposite hypotheses for impacts of climate shifts. A) Increased dust emission with increased
15 aridity and reduced vegetation coverage. B) Emission will decrease under drier, less stormy
16 climate as less sediments replenish dust sources by floods. Here we test these hypotheses by
17 analyzing an ~11-m long core, archiving Holocene dust, trapped in the Montezuma Well (MW),
18 Arizona, together with current dust sources and transport pathways. Major elements indicate that
19 MW sediments originated from two end-members: local carbonate bedrock and external silicate-
20 rich dust. Core sediments are similar to the adjacent silicate-rich soils accumulated over the
21 carbonates, pointing to their eolian origin. Particle-size distributions reveal that the accumulating
22 dust in the core are fine and coarse dust, respectively transported during winters and summers
23 from eastern Arizona and Mojave Desert and from southern Arizona, similar to current climate
24 systems and dust pathways. Surveys of potential dust sources indicate that current summer and
25 winter dust sources are supply-limited and transport-limited fluvial systems, respectively. Dust

26 fluxes were high during the wetter phases of the Holocene when winter sources dominated.
27 During the middle Holocene drought, dust fluxes were minimal, dominated by summer sources
28 up to shut down as drought conditions did not produce enough floods to refill these sources with
29 entrainable sediments. We propose that in semiarid central Arizona, dust activity is strongly
30 connected with climate, occurring primarily during humid intervals, and enhanced by dust
31 supplied by replenishing of sediments at dust sources.

32 **INTRODUCTION**

33 Associating climatic conditions with dust emission, transport, and deposition in aridlands
34 remains indistinct. Two opposite hypotheses prevail for climate shifts from relatively humid to
35 more arid or even towards drought. The common hypothesis involves increased dust emission
36 with declining vegetation coverage at dust sources (Middleton, 1985; McTainsh et al., 2005;
37 Cook et al., 2009; Marx et al., 2009) considered availability-limited sources. Opposite hypothesis
38 assumes that under drier conditions, lacking storms usually associated with wetter conditions,
39 dust emission decreases as sediments do not replenish the sources by occasional flooding (i.e.,
40 supply-limited and/or transport-limited sources) (Bullard and Livingstone, 2002; Routson et al.,
41 2016; Arcusa et al., 2019); furthermore, a lack of storms may also indicate less windstorms.

42 Dust storms in the Sonoran Desert (Arizona, USA) are frequent, leading to fatal car accidents
43 and health problems (Raman et al., 2014). Whereas the synoptic climatology of dust storms in
44 Arizona is relatively known (Nickling and Brazel, 1984; Brazel et al., 1986), the geomorphic
45 nature of dust sources in this region, and their response to changing climate, is practically
46 unknown, both for the present and for the Holocene. During the Younger Drays (YD, 12.9-11.7
47 ka) and the early Holocene (11.7-8.2 ka), climate was characterized by high rainfall, changing to
48 warmer and drier climate, known as the Middle Holocene Drought (MHD, 8.2-4.2 ka; e.g.,

49 Lachniet et al., 2020; Thompson et al., 1993), and switched to a wetter climate towards the late
50 Holocene (<4.2 ka) (Kirby et al., 2015). Therefore, this area can serve as an ideal test of the
51 opposing hypotheses of climate-dust relationships. To do so, we analyzed flux and properties of
52 dust recorded by an 11.25-m-long Holocene sediment core retrieved from Montezuma Well
53 (MW), central Arizona (Fig. 1) (Davis and Shafer, 1992). The MW is a perfect dust trap, with
54 carbonate bedrock that stands out against the silicate-rich prevailing regional dust, and without
55 fluvial input. Together with analyses of current dust sources and transport pathways, i.e.,
56 potential analogs for the Holocene dust sources and pathways, we evaluate the relationships
57 between Holocene climate and dust at the millennial time scale.

58 **RESEARCH AREA AND METHODS**

59 The MW is a natural, circular-shape (108 m diameter) sinkhole filled with deep water (~16 m),
60 located at the northern edge of the Sonoran Desert (Fig.1), surrounded by Miocene–early
61 Pliocene limestone and travertine of the Verde Formation (Donchin, 1983). Current dust
62 pathways are associated with winter cyclones and the North American Monsoon (NAM) (Adams
63 and Comrie, 1997; Sheppard et al., 2002). The cyclones transport dust from the west, mainly
64 during winter and the NAM from the southwest–southeast, mainly during summer (Nickling and
65 Brazel, 1984).

66 Modern dust pathways were estimated by HYSPLIT-back trajectory model on 17 high dust
67 concentration days (Table S1). Current dust sources in the region were identified using MODIS
68 deep blue aerosol remote sensing data (Ginoux et al., 2012) ;We sampled and described the
69 matching current dust pathway (total of 15 individual sources, 41 samples). A core was retrieved
70 in 1985 from the northwest part of MW to avoid influence of spring discharge (Davis and Shafer,
71 1992). We collected 84 samples from the core and sampled the local bedrock (seven samples)
72 and two adjacent soil profiles (six samples) (Fig S1). Age control was established using eight

73 C14 samples combined with published six C14 ages (Davis and Shafer, 1992). Age-depth model
74 was processed using Bacon modelling package (Blaauw & Christeny, 2011; Table S2; Fig. S2).
75 Bulk density was determined following Blake (1965). Major element concentrations of the core,
76 bedrock, soils, and current dust sources samples were analyzed using an ICP-OES. Chemical
77 scores were estimated by projecting MW core samples on calculated mixing lines (Data
78 Repository). Particle-Size Distributions (PSD) of the core, soils and current dust sources samples
79 were analyzed following Crouvi et al. (2008). Core samples were treated to remove carbonate
80 and organic matter (Arcusa et al., 2019) before analysis and thus represent deposited dust (Data
81 Repository). Dust PSD was unmixed to individual end members (Ems) using AnalySize
82 MATLAB GUI package (Paterson and Heslop, 2015), an End Member Modeling Analysis
83 (EMMA) software. Total dust and bedrock fluxes were calculated using Al and Ca contents,
84 respectively, and C14 ages (Equations 1, 2 in Data Repository). Dust fluxes of individual EMs
85 were calculated by multiplying total dust flux by the PSD EM score.

86 **RESULTS**

87 Unsurprisingly, current dusty days reveal two distinct dust transport pathways: (a) summer
88 storms related to the NAM with air mass transporting mainly from the southwest and south, and
89 (b) winter storms from the west and northwest (Fig 1). All identified current dust sources located
90 along these pathways, are distinct geomorphic units related to fluvial systems (Data Repository).
91 Thus, these sources are considered supply-limited sources. Sources along summer dust pathways
92 (herein summer sources) are washes, floodplains, and alluvial fans. The washes (NH, UT, and
93 CE) are wide (~1 km), with low vegetation and gravel cover (<20%), and a silt clay loam to loam
94 texture. The Gila River floodplains (PL) are few km wide with 20-30% vegetation coverage that
95 currently are cultivated; surficial sediments are silt loam to sandy loam. The alluvial fans (rest of
96 summer sources) are composed of 1-5 m wide washes and terraces with low vegetation (10-30%)

97 and gravel (~5%) cover; sediments are silt loam to loamy sand. The PSDs of the summer sources
98 are mostly unimodal, with modes at $35 \pm 22 \mu\text{m}$ (n=7), $61 \pm 20 \mu\text{m}$ (n=5) and $76 \pm 24 \mu\text{m}$ (n=21)
99 for the washes, floodplains, and alluvial fans, respectively. Dust sources along winter dust
100 pathways (herein winter sources) are playas and floodplains. Kingman playa (KG) is a circular
101 (~65 km²) basin drained by an active wash; surface is bare, with a well-developed crust of silt
102 clay to silt loam sediments. The Colorado River floodplains (BH), used for agricultural, are 2-3
103 km wide with 20% vegetation cover; surficial sediments are clay loam to silt loam. These winter
104 sources are finer than the summer sources, exhibiting unimodal PSDs with modes at $25 \pm 19 \mu\text{m}$
105 (n=2) and $16 \pm 14 \mu\text{m}$ (n=5) for the BH and KG, respectively.

106 Soil profiles adjacent to MW are shallow (~12 cm thick) brown lithosols with no clear horizons,
107 and a sharp and clear contact with the carbonate bedrock. Texture is silty clay loam to silt loam
108 with unimodal PSD; average mode is $24 \pm 12 \mu\text{m}$ (n=6), and topsoil mode is $32 \mu\text{m}$ (Fig. 2);
109 carbonate clasts are ~10%, mainly in the lower part.

110 The core sediments are silt to silt loam, containing variable amounts of roots and twigs, rock
111 fragments, snails, and clams. The new C14 ages extend the published C14 ages to 13-1.2 cal ka
112 BP (Table S2). The age-depth model (Fig. S2) reveals that accumulation rates were highest
113 during the late Holocene (0.24 cm/yr), intermediate during the YD and the early Holocene (0.10-
114 0.14 cm/yr), and lowest during the MHD (0.02 cm/yr). The PSDs of the core are mostly
115 unimodal with modes from 11-66 μm , showing a general coarsening upwards trend and an
116 average mode of $36 \pm 13 \mu\text{m}$ (n=49), similar to an adjacent soil (Fig. 2). The EMMA reveals
117 three distinct dust modes (Fig. 2), at 13 μm (EM1), 34 μm (EM2), and 75 μm (EM3). The two
118 higher EMs are coarse dust and EM1 is fine dust. The scores of these two dust fractions (EM1
119 and EM2+3) oscillate in the lower parts of the core during the YD (Fig. 4), but towards and

120 during the MHD, the coarse fraction (EM2+3) dominates the PSD, a pattern that continues also
121 during the late Holocene.

122 The core samples lie along a mixing line between two distinct compositions (Fig. 3): (a) local
123 bedrock, Ca rich and Al and Fe poor, and (b) dust, Ca poor and Al and Fe rich, represented by
124 samples taken from current dust sources in Arizona (this study) and from the Mojave Desert
125 (Reheis et al., 2009). Summer and winter sources slightly differ in their Al-Ca-Fe values; winter
126 sources resemble the Mojave Desert values. Similar to the core sediments, the adjacent soils lie
127 along this mixing line, but closer to the bedrock composition. Calculated winter/summer scores
128 reveal low values of winter dust during the YD, switching towards high values during the early
129 Holocene, an opposite trend to the PSD scores (Fig 4). Summer dust dominates the rest of the
130 core, resembling the PSD scores.

131 Total dust flux is high (0.2-0.4 g/cm²/yr) during the YD and early Holocene (Fig 4), dominated
132 by fine dust (EM1). Towards and during the MHD, total dust flux dramatically decreases to the
133 lowest recorded fluxes (0.01-0.1 g/cm²/yr), originated mostly from coarse dust (EM 2+3). Total
134 flux increased towards late Holocene, dominated by coarse dust. Pulses of MW escarpment
135 contribution (Fig 4) are not correlated with dust fluxes and show high values at 9.5, 7 and 2 ka,
136 in accordance with rock fragments in the core.

137 **DISCUSSION**

138 **Dust Sources in Central Arizona**

139 The similarity between the PSD and chemical compositions of the core and soils supports our
140 assumption that the siliceous sediments in the core are of external origin. Moreover, the three
141 calculated PSD EMs of the core generally fit the PSDs of surficial sediments sampled in current
142 dust sources: The coarse EMs fit the summer sources located 180-300 km south and southwest of
143 MW (EM2 fit the washes and EM3 fit the alluvial fans and Gila River floodplains). The fine EM

144 fits winter sources (Kingman Playa and Colorado River floodplain) located 2270 30 km west and
145 northwest of MW. The PSDs of Mojave Desert dust sources vary (Reheis et al., 2009), but given
146 their relatively long transport distance (~400 km; Fig. 1), we consider them as contributing
147 mainly to EM1. Furthermore, Mojave Desert sources are chemically similar to the winter sources
148 in Arizona (Fig 3).

149 Independent observations support these interpretations: Modern dust traps in eastern Colorado
150 Plateau have higher amounts of <10 μm dust at winters compared with coarser dust at summers
151 (Reheis & Urban, 2011). Fine dust was observed being transported at least 400 km from western
152 Mojave Desert eastwards towards Arizona (Reheis et al., 2002), whereas coarse dust settles
153 within few tens of kilometers (Reheis & Rolf, 1995). Finally, theoretical relationship between
154 wind properties and grain size indicates that 35-60 μm grains travel 180-300 km only during
155 intensive haboob- type storms (Tsoar and Pye, 1987) that are typical to the NAM, but are absent
156 in current winter dust storms (Raman et al., 2014). Thus, only fine dust from the Mojave Desert
157 can reach MW under current winter storms conditions; coarse dust can be transported to MW
158 during haboobs that characterize the NAM.

159 **Temporal Changes in Dust Flux**

160 Dust fluxes during the YD are the highest (Fig. 4), matching reconstructed dust fluxes in the
161 Colorado Plateau (Arcusa et al., 2019). We propose that these high fluxes are related to the
162 gradual drying of lakes in the Mojave Desert during deglaciation (Enzel et al., 2003), exposing
163 erodible sediments and changing these basins into transport-limited dust sources. Frequent winter
164 storms, related to a more southern position of the polar jet, resulted in increased rainfall and
165 flooding replenishing these sources (Enzel et al., 2003; Asmerom et al., 2010). During the early
166 Holocene dust fluxes decreased to about one half of the YD values (Fig. 4), and were dominated

167 by summer sources, indicating increased NAM and decreased winter dust pathways. Climate
168 remained relatively humid, and NAM increasingly dominating (Kirby et al., 2015). The
169 transition towards and during the MHD was associated with an increase of the NAM activity and
170 a decrease in winter storms (Metcalf et al., 2015), which portrays an arid climate (Davis and
171 Shafer, 1992; Macdonald et al., 2016; Lachniet et al., 2020). At MW, total dust fluxes became
172 extremely low (Fig. 4). These conditions led to drying of the Mojave Desert lakes, transforming
173 them to supply-limited (dry playas) (Enzel et al., 2003), or availability-limited (wet playas)
174 sources (Reynolds et al., 2007). This shift can explain the gradual decrease in dust flux. At that
175 time, coarse dust (Reynolds et al., 2006) and low dust fluxes (Arcusa et al., 2019) were observed
176 in the Colorado Plateau. Towards the late Holocene, the area experienced wetter and colder
177 conditions (Polyak and Asmerom, 2001; Kirby et al., 2015) resulting in higher dust fluxes,
178 dominated by summer, supply-limited sources. At that time, increased episodes of alluvial
179 activity were documented (e.g., Harden et al., 2010).

180 Throughout the YD and early Holocene, PSD and chemistry scores are uncorrelated. A probable
181 explanation is that the higher rainfall during the YD and early Holocene increased partial
182 leaching of elements at dust sources.

183 **Drought Decreases Dust Emission**

184 During the MHD, dust fluxes are minimal and dust sources in the region, both winter and
185 summer, are in supply-limited state. We propose that the low frequency of storms resulted in
186 lower-frequency of floods and windy days, and therefore, negligible supply of sediments to the
187 fluvial systems; thus, shutting off these supply-limited dust sources. Action of water is crucial for
188 creating dust, as fluvial systems supply weathered sediments that settle on top of alluvial fans,
189 washes, and playas, where they dry and become available for eolian transport. Our findings

190 reinforce the conceptual framework of Bullard and Livingstone (2002) that supply-limited dust
191 sources boost production during relatively humid climate, and are less active during drought
192 intervals.

193 **SUMMARY**

194 The MW records changing Holocene dust fluxes and sources, revealing millennial-scale
195 summer/winter paleoclimate reconstruction for central Arizona. The middle Holocene drought
196 shut off the supply-limited dust sources, generating very low dust accumulation rates. Our study
197 shows that dust activity in Southwestern USA is controlled by the combination of wet-to-arid
198 climate and the paleohydrology of dust sources, i.e., whether they are supply-, availability-, or
199 transport-limited. Thus, studies of current and paleo dust should account for the relationship
200 between these two factors for characterizing and estimations of dust activity at a given region.

201 **ACKNOWLEDGMENTS**

202 This research was supported by Israel Science Foundation (grant no. 1672/15) and US-Israel
203 Binational Science Foundation (grant no. 2014341).

204 ¹GSA Data Repository item 201Xxxx, includes method and raw data description of MW core
205 and its geological endmembers, is available online at www.geosociety.org/pubs/ft20XX.htm, or
206 on request from editing@geosociety.org.

207 **FIGURE CAPTIONS**

208 Figure 1. A. The main physiographic units in the SW USA, Montezuma Well (MW) location,
209 and current dust transport pathways. B. Topographic map of the study area with main cities and
210 rivers, current dust sources identified using remote sensing and classified by their geomorphic
211 nature, and samples location and name (Data repository). Identified current dust transport
212 pathways are marked (summer-red, winter-blue). C. Photo of MW.

213 Figure 2. The PSDs of MW core (black is average, yellow range is standard deviation), adjacent
214 topsoil (dashed black), and the three EMMA endmembers. Inset: Summer fit includes PSD of

215 MW summer EM (dashed red) results from EMMA and summer dust sources (black), from right
216 to left – alluvial fan (GR), flood plain (PL) and wash (NH). Winter fit includes MW winter EM
217 (dashed blue) and winter dust sources (black), from right to left – flood plain (BH) and playa
218 (KG).

219 Figure 3. Triangular plot Ca-Al-Fe. All MW samples and adjacent soil (S) lay along two mixing
220 lines between the bedrock and the summer and winter dust endmembers.

221 Figure 4. A. The MW stratigraphy chart (rock fragments- gray); B. Aridity index estimated from
222 archives in the SW USA (Lachniet et al., 2020); C. The PSD EMs calculated by EMMA; D.
223 Chemistry scores calculated based on Fig. 3; E.D. Total dust flux and PSD EMs fluxes, and F.
224 Bedrock flux.

225 REFERENCES CITED

- 226 1. Adams, D.K., and Comrie, A.C., 1997, The North American Monsoon: Bulletin of the
227 American Meteorological Society, v. 78, p. 2197–2213, doi:10.1175/1520-
228 0477(1997)078<2197:TNAM>2.0.CO;2.
- 229 2. Arcusa, S.H., McKay, N.P., Routson, C.C., and Munoz, S.E., 2019, Dust-drought
230 interactions over the last 15 , 000 years : A network of lake sediment records from the
231 San Juan Mountains , Colorado: The Holocene, doi:10.1177/0959683619875192.
- 232 3. Asmerom, Y., Polyak, V.J., and Burns, S.J., 2010, Variable winter moisture in the
233 southwestern United States linked to rapid glacial climate shifts: Nature Geoscience, v. 3,
234 p. 114–117, doi:10.1038/ngeo754.
- 235 4. Blaauw, M., and Christeny, J.A., 2011, Flexible paleoclimate age-depth models using an
236 autoregressive gamma process: Bayesian Analysis, v. 6, p. 457–474, doi:10.1214/11-
237 BA618.
- 238 5. Blake, G.R., 1965, Bulk Density 1: Methods of soil analysis. Part 1. Physical and
239 mineralogical properties, including statistics of measurement and sampling, p. 374–390.

- 240 6. Brazel, A.J., Nickling, W.G., and Lee, J., 1986, Effect of antecedent moisture conditions
241 on dust storm generation in Arizona: *Aeolian Geomorphology*, Proceedings of the 17th
242 Annual Binghamton Symposium, p. 261–271.
- 243 7. Bullard, J.E., and Livingstone, I., 2002, Interactions systems between aeolian and fluvial
244 in dryland environments: *Area*, v. 34, p. 8–16.
- 245 8. Cook, B.I., Miller, R.L., and Seager, R., 2009, Amplification of the north american “Dust
246 Bowl” drought through human-induced land degradation: *Proceedings of the National
247 Academy of Sciences of the United States of America*, v. 106, p. 4997–5001,
248 doi:10.1073/pnas.0810200106.
- 249 9. Crouvi, O., Amit, R., Enzel, Y., Porat, N., and Sandler, A., 2008, Sand dunes as a major
250 proximal dust source for late Pleistocene loess in the Negev Desert, Israel: *Quaternary
251 Research*, v. 70, p. 275–282, doi:10.1016/j.yqres.2008.04.011.
- 252 10. Davis, O.K., and Shafer, D.S., 1992, A Holocene climatic record for the Sonoran Desert
253 from pollen analysis of Montezuma Well, Arizona, USA: *Palaeogeography,
254 Palaeoclimatology, Palaeoecology*, v. 92, p. 107–119, doi:10.1016/0031-0182(92)90137-
255 T.
- 256 11. Donchin, J.H., 1983, *Stratigraphy and Sedimentary Environments of the Miocene-
257 Pliocene Verde Formation in the Southeastern Verde Valley, Yavapai County, Arizona:
258 [Ph.D. thesis]:Northern Arizona University.*
- 259 12. Enzel, Y., Wells, S.G., and Lancaster, N., 2003, Late Pleistocene lakes along the Mojave
260 River, southeast California: *Special Paper of the Geological Society of America*, v. 368,
261 p. 61–77, doi:10.1130/0-8137-2368-X.61.
- 262 13. Ginoux, P., Prospero, J.M., Gill, T.E., Hsu, N.C., and Zhao, M., 2012, Global-scale

- 263 attribution of anthropogenic and natural dust sources and their emission rates based on
264 MODIS Deep Blue aerosol products: *Reviews of Geophysics*, v. 50,
265 doi:10.1029/2012RG000388.
- 266 14. Harden, T., Macklin, M.G., and Baker, V.R., 2010, Holocene flood histories in south-
267 western USA: *Earth Surface Processes and Landforms*, v. 35, p. 707–716,
268 doi:10.1002/esp.1983.
- 269 15. Kirby, M.E. et al., 2015, Evidence for insolation and Pacific forcing of late glacial
270 through Holocene climate in the Central Mojave Desert (Silver Lake, CA): *Quaternary*
271 *Research (United States)*, v. 84, p. 174–186, doi:10.1016/j.yqres.2015.07.003.
- 272 16. Lachniet, M.S., Asmerom, Y., Polyak, V., and Denniston, R., 2020, Great Basin
273 Paleoclimate and Aridity Linked to Arctic Warming and Tropical Pacific Sea Surface
274 Temperatures: *Paleoceanography and Paleoclimatology*, v. 35, p. 1–22,
275 doi:10.1029/2019PA003785.
- 276 17. Macdonald, G.M., Moser, K.A., Bloom, A.M., Potito, A.P., Porinchu, D.F., Holmquist,
277 J.R., Hughes, J., and Kremenetski, K. V., 2016, Prolonged California aridity linked to
278 climate warming and Pacific sea surface temperature: *Scientific Reports*, v. 6, p. 1–8,
279 doi:10.1038/srep33325.
- 280 18. Marx, S.K., McGowan, H.A., and Kamber, B.S., 2009, Long-range dust transport from
281 eastern Australia: A proxy for Holocene aridity and ENSO-type climate variability: *Earth*
282 *and Planetary Science Letters*, v. 282, p. 167–177, doi:10.1016/j.epsl.2009.03.013.
- 283 19. McTainsh, G., Chan, Y.C., McGowan, H., Leys, J., and Tews, K., 2005, The 23rd
284 October 2002 dust storm in eastern Australia: Characteristics and meteorological
285 conditions: *Atmospheric Environment*, v. 39, p. 1227–1236,

- 286 doi:10.1016/j.atmosenv.2004.10.016.
- 287 20. Metcalfe, S.E., Barron, J.A., and Davies, S.J., 2015, The Holocene history of the North
288 American Monsoon : ‘ known knowns ’ and ‘ known unknowns ’ in understanding its
289 spatial and temporal complexity: *Quaternary Science Reviews*, v. 120, p. 1–27,
290 doi:10.1016/j.quascirev.2015.04.004.
- 291 21. Middleton, N.J., 1985, Dust production in the Sahel (reply): *Nature*, v. 318, p. 488,
292 doi:10.1038/318488b0.
- 293 22. Nickling, W.G., and Brazel, A.J., 1984, Temporal and spatial characteristics of Arizona
294 dust storms (1965- 1980): *Journal of Climatology*, v. 4, p. 645–660.
- 295 23. Paterson, G.A., and Heslop, D., 2015, *Geochemistry, Geophysics, Geosystems*: , p.
296 4494–4506, doi:10.1002/2015GC006070.Received.
- 297 24. Polyak, V.J., and Asmerom, Y., 2001, Late Holocene climate and cultural changes in the
298 southwestern United States: *Science*, v. 294, p. 148–151, doi:10.1126/science.1062771.
- 299 25. Raman, A., Arellano, A.F., and Brost, J.J., 2014, Revisiting haboobs in the southwestern
300 United States: An observational case study of the 5 July 2011 Phoenix dust storm:
301 *Atmospheric Environment*, v. 89, p. 179–188, doi:10.1016/j.atmosenv.2014.02.026.
- 302 26. Reheis, M.C., Budahn, J.R., and Lamothe, P.J., 2002, Geochemical evidence for diversity
303 of dust sources in the southwestern United States RN - *Geochim. Cosmochim. Acta*, v.
304 66, no. 9, p. 1569-1587: *Geochim.Cosmochim. Acta*, v. 66, p. 1569–1587,
305 doi:10.1016/S0016-7037(01)00864-X.
- 306 27. Reheis, M.C., Budahn, J.R., Lamothe, P.J., and Reynolds, R.L., 2009, Compositions of
307 modern dust and surface sediments in the Desert Southwest, United States: *Journal of*
308 *Geophysical Research: Earth Surface*, v. 114, p. 1–20, doi:10.1029/2008JF001009.

- 309 28. Reheis, M.C., and Rolf, K., 1995, Dust deposition in southern Nevada and California,
310 1984-1989: Relations to climate, source area, and source lithology: *Journal of*
311 *Geophysical Research*, v. 100, p. 8893–8918.
- 312 29. Reheis, M.C., and Urban, F.E., 2011, Regional and climatic controls on seasonal dust
313 deposition in the southwestern U.S.: *Aeolian Research*, v. 3, p. 3–21,
314 doi:10.1016/j.aeolia.2011.03.008.
- 315 30. Reynolds, R.L., Reheis, M.C., Neff, J.C., Goldstein, H., and Yount, J., 2006, Late
316 Quaternary eolian dust in surficial deposits of a Colorado Plateau grassland: Controls on
317 distribution and ecologic effects: *Catena*, v. 66, p. 251–266,
318 doi:10.1016/j.catena.2006.02.003.
- 319 31. Reynolds, R.L., Yount, J.C., Reheis, M.C., Goldstein, H., Pat Chavez, J., Robert Fulton,
320 John Whitney, Christopher Fuller, and Richard M. Forester, 2007, Dust Emission from
321 Wet and Dry Playas in the Mojave Desert, USA: *Earth Surface Processes and Landforms*,
322 v. 32, p. 1811–1827, doi:10.1002/esp.1515.
- 323 32. Routson, C.C., Overpeck, J.T., Woodhouse, C.A., and Kenney, W.F., 2016, Three
324 millennia of southwestern north American dustiness and future implications: *PLoS ONE*,
325 v. 11, p. 11–12, doi:10.1371/journal.pone.0149573.
- 326 33. Sheppard, P.R., Comrie, A.C., Packin, G.D., Angersbach, K., and Hughes, M.K., 2002,
327 The climate of the US Southwest: *Climate Research*, v. 21, p. 219–238,
328 doi:10.3354/cr021219.
- 329 34. Thompson, R.S., Whitlock, C., Bartlein, P.J., Harrison, S.P., Spaulding, W.G., Wright,
330 H.E., Kutzbach, J.E., Webb, T.I.I.I. and Ruddiman, W.F., 1993, Climatic changes in the
331 western United States since 18,000 yr BP. *Global climates since the last glacial*

332 maximum. 1993 Jun 1:468-513.: Global climates since the last glacial maximum, v. 1, p.
333 468–513.

334 35. Tsoar, H., and Pye, K., 1987, Dust transport and the question of desert loess formation:
335 Sedimentology, v. 34, p. 139–153, doi:10.1111/j.1365-3091.1987.tb00566.x.

336

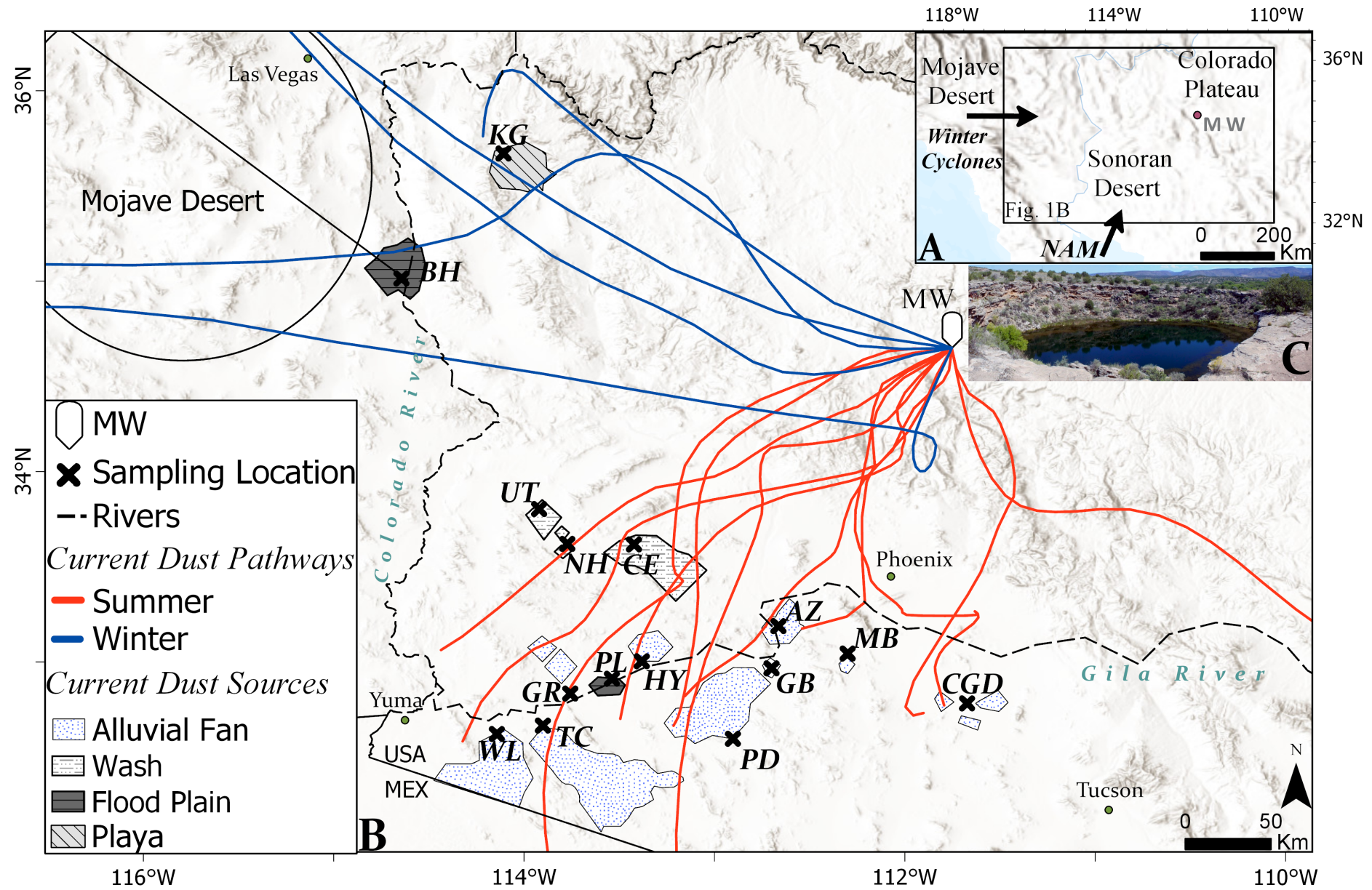


Figure 1. A. The main physiographic units in the SW USA, Montezuma Well (MW) location, and current dust transport pathways. B. Topographic map of the study area with main cities and rivers, current dust sources identified using remote sensing and classified by their geomorphic nature, and samples location and name (Data repository). Identified current dust transport pathways are marked (summer-red, winter-blue). C. Photo of MW.

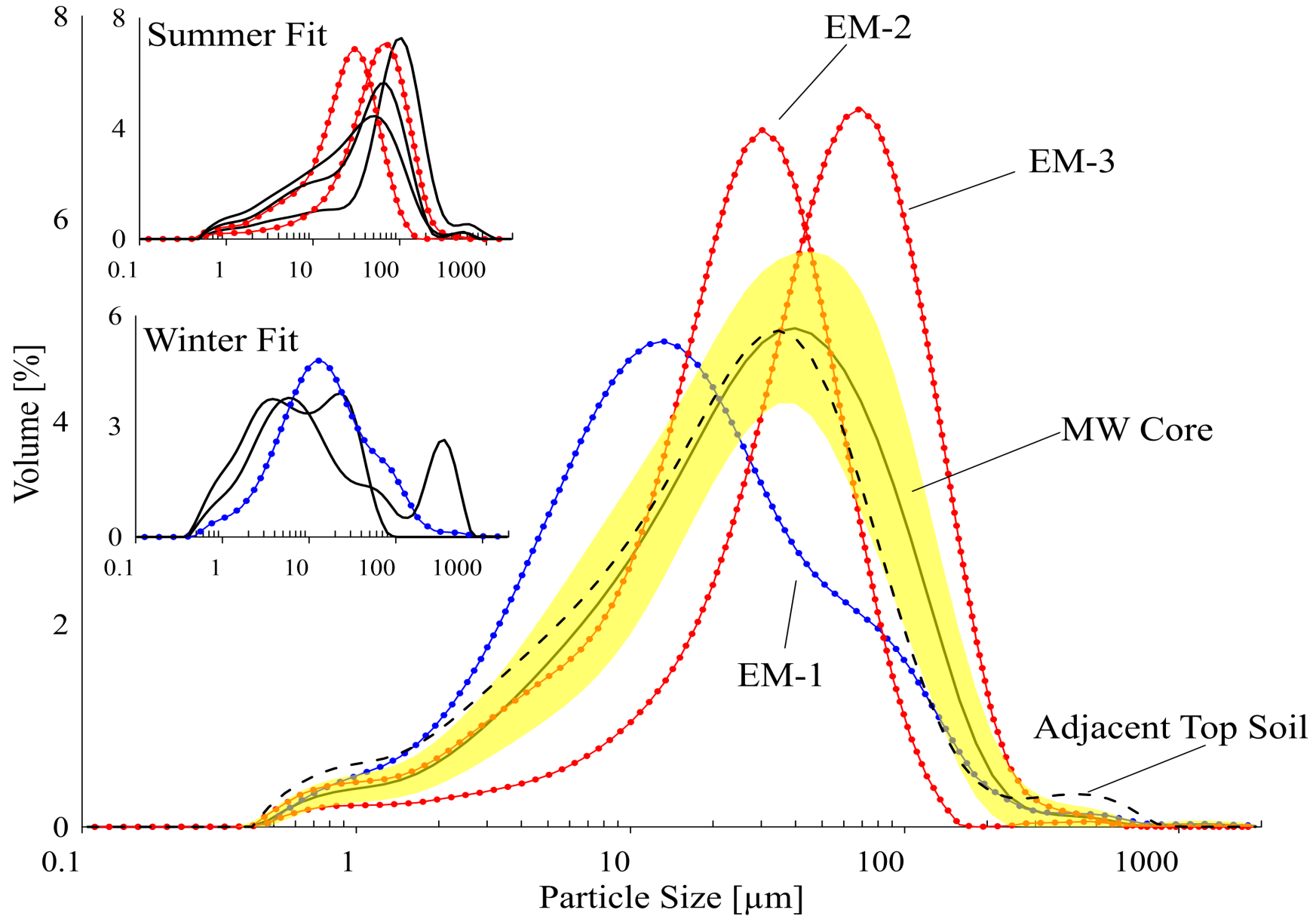


Figure 2. The PSDs of MW core (black is average, yellow range is standard deviation), adjacent topsoil (dashed black), and the three EMMA endmembers. Inset: Summer fit includes PSD of MW summer EM (dashed red) results from EMMA and summer dust sources (black), from right to left – alluvial fan (GR), flood plain (PL) and wash (NH). Winter fit includes MW winter EM (dashed blue) and winter dust sources (black), from right to left – flood plain (BH) and playa (KG).

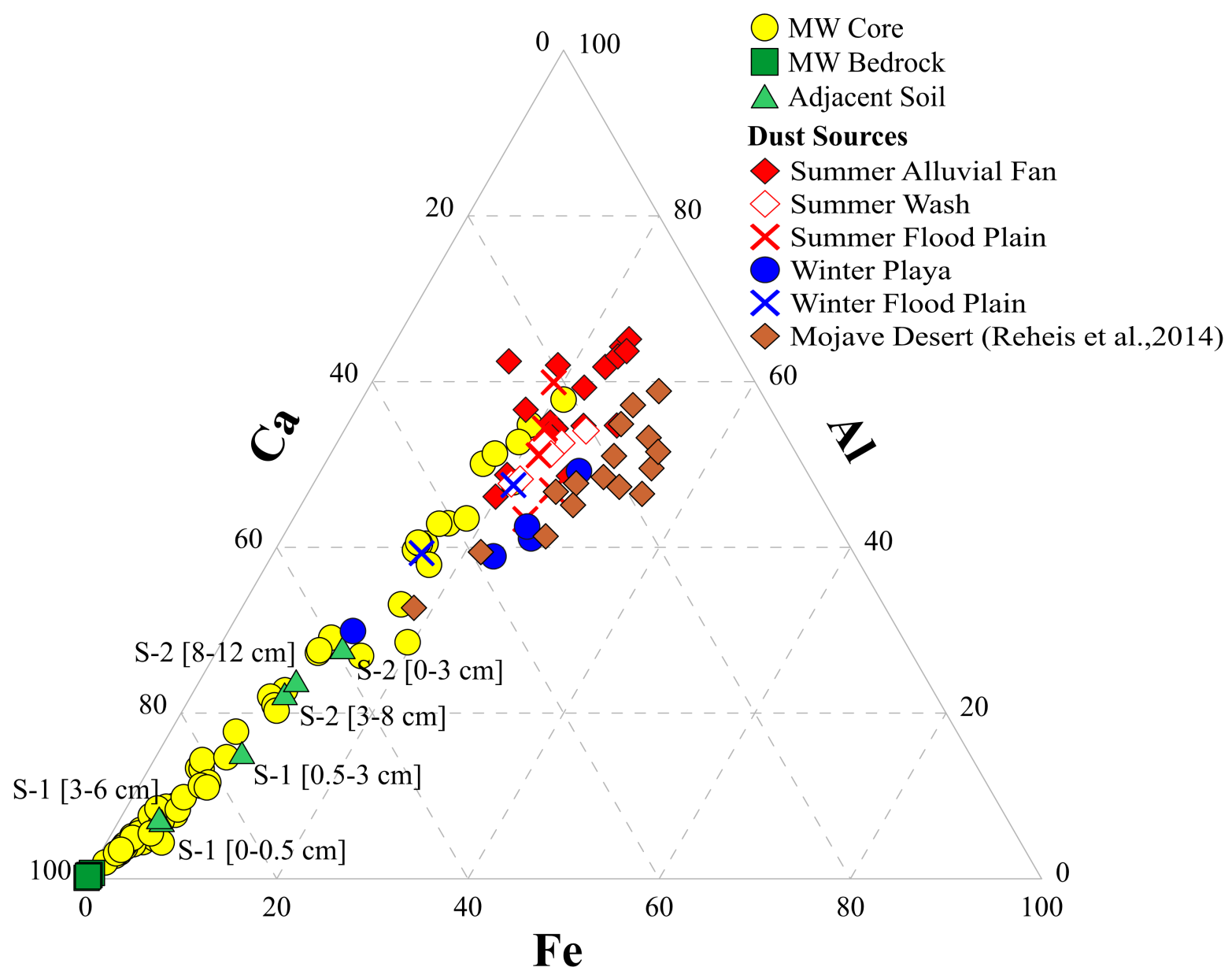


Figure 3. Triangular plot Ca-Al-Fe. All MW samples and adjacent soil (S) lay along two mixing lines between the bedrock and the summer and winter dust endmembers.

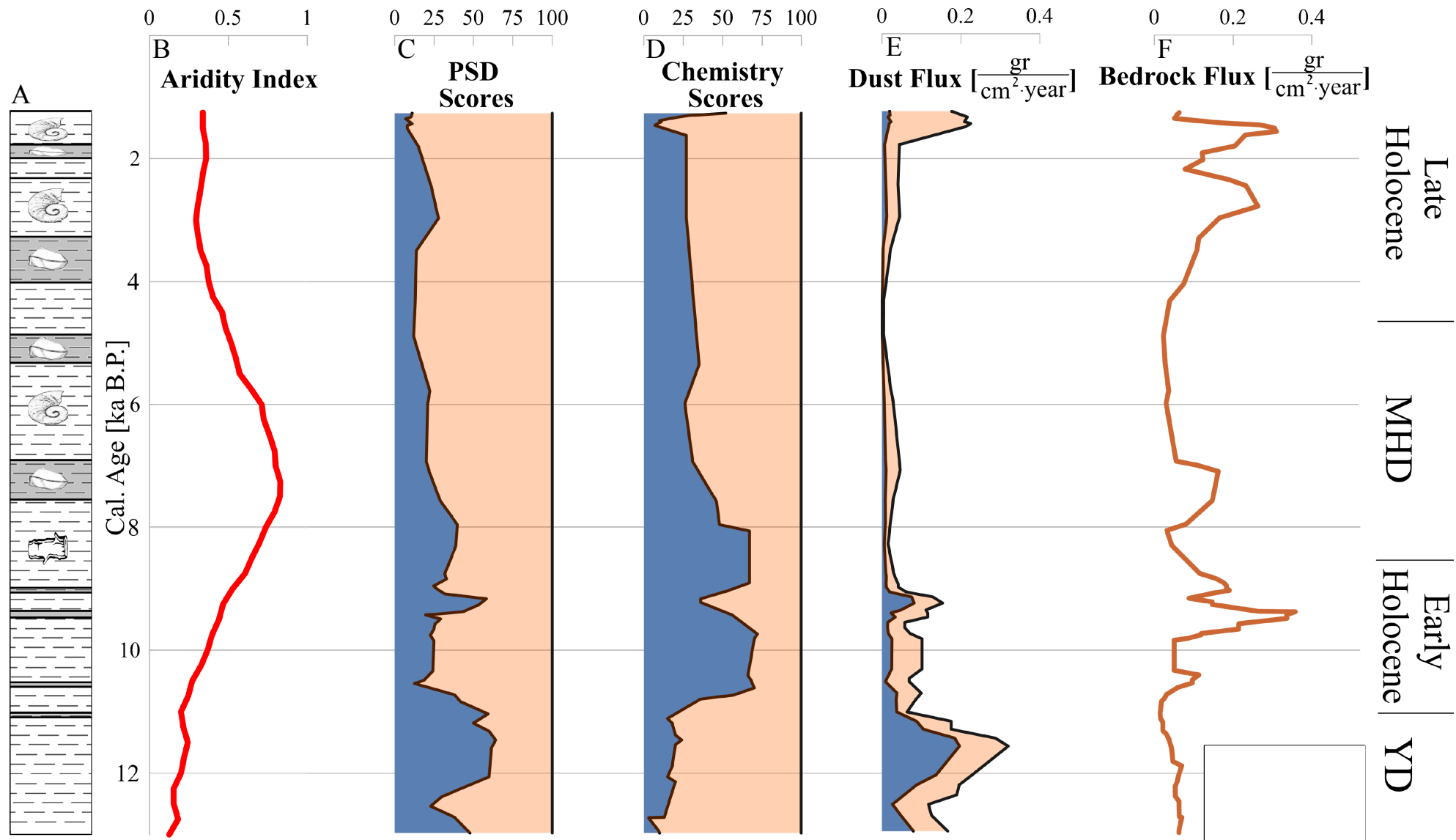


Figure 4. A. The MW stratigraphy chart (rock fragments- gray); B. Aridity index estimated from archives in the SW USA (Lachniet et al., 2020); C. The PSD EMs calculated by EMMA; D. Chemistry scores calculated based on Fig. 3; E.D. Total dust flux and PSD EMs fluxes, and F. Bedrock flux.